

# **A SOLID-STATE C-BAND POWER AMPLIFIER FOR COMMUNICATIONS SATELLITES**

**J. Nicholas LaPrade  
RCA Astro-Electronics  
Princeton, New Jersey**

## **ABSTRACT**

A solid-state power amplifier now routinely replaces the traveling-wave tube amplifier in C-band communications satellites. The immediate benefit of superior performance is realized by increased transponder capacity. Long-term benefits of higher reliability and reduced production costs are also projected.

This paper describes salient features of the first solid-state power amplifier to fully replace the traveling-wave tube amplifier in spaceborne transponders. The 8.5-watt, 60-dB gain amplifier employs a chain of gallium-arsenide field-effect transistors to provide a 160-MHz usable bandwidth within the 3.7- to 4.2-GHz downlink band. Data typical for this amplifier are presented. The key parameters of efficiency, intermodulation distortion, and phase effects are described in detail.

The amplifier is being manufactured for numerous communications satellite programs. Aspects of reproducibility and automated testing at the various stages of amplifier production are addressed. Forty-eight amplifiers are now operational at geosynchronous altitude with several times that number scheduled for launch within the next few years.

## **INTRODUCTION**

The solid-state power amplifier (SSPA) described herein is the result of a joint development effort between RCA Laboratories and RCA Astro-Electronics. The SSPA was designed specifically to replace an 8.5-watt traveling-wave tube amplifier (TWTA) in C-band satellite transponders. Comparison of the TWTA and SSPA shows the SSPA to be lighter in weight and more linear at all points of the amplitude and phase characteristics. These advantages, coupled with greater reliability inherent for solid-state technology, far outweigh the slightly lower saturated dc-to-rf efficiency of the SSPA.

The SSPA has proven to be quite manufacturable. Over 100 units have been assembled and tested with a very high degree of reproducibility. Data for seven amplifiers

demonstrated efficiencies from 32% to 35% with typical gain above 62 dB and average  $C/IM_3$  at operating point of -13 dBc for the two-tone measurement.<sup>(1)</sup>

## SSPA DESIGN

The amplifier is a six-stage design. A block diagram is given in Figure 1. The first four single-ended stages comprise the high-gain driver section. The last two stages are balanced amplifiers configured using the power devices between interdigitated quadrature hybrids. The driver section is capable of 0.5 watt output across the full 500-MHz band with typical small-signal gain in excess of 47 dB. The power section has a saturated power output capability in excess of 10 watts and typical operating point gain greater than 15 dB over a 160-MHz bandwidth.

The four paralleled output stages use a Fujitsu FLC30 device selected for high efficiency. The nominal input of 0.5 watt results in at least a 2.5-watt power output with typical power-added efficiency of 40%. Device thermal resistance is typically 11 °C/W with additional resistance of 3 °C/W in the heat sinking.

Assuming a nominal spacecraft panel temperature of 45 °C results in a calculated channel temperature of

$$T_{CH} = 45^{\circ}\text{C} + (11^{\circ}\text{C/W} + 3^{\circ}\text{C/W})3\text{W} = 87^{\circ}\text{C}$$

Channel temperatures below 110 °C are essential to a 10-year operational life. The FLC30 device, as for all other GaAs FET devices in this design, is impedance matched to 50 ohms using microstrip techniques on alumina substrate. Because the device is operated primarily into gain compression, the small-signal S-parameters are insufficient to achieve an optimum circuit design. The output circuit was designed using a novel load-pull technique that characterizes the trade-off between power output and linearity.<sup>(2)</sup> Once output microstrip circuit geometry is realized using load-pull data with a CAD optimization routine, the small-signal S-parameter data are used in conjunction with the established output circuit to redesign the final input matching network. Careful implementation of this design approach minimizes the number of iterations required for optimum matching.

The driver amplifier section provides high gain to the 0.5-watt level for the SSPA power section. The first three GaAs FET amplifier stages are nested between isolators to permit alignment for maximum gain flatness and minimum gain slope. Uncompensated, the entire SSPA gain can vary as much as 5 dB p-p over a 40 °C temperature range. Unique compensation circuitry within the driver section is employed to reduce this variation to 1.3 dB p-p, maximum. Measured GaAs FET gain versus gate voltage characteristics are used in a computer program along with standard amplifier and thermistor thermal

characteristics to select the correct bias compensation points. Correlation between predicted and actual results has been quite consistent.

## AMPLIFIER TESTING

Each amplifier is flight acceptance tested prior to delivery to the spacecraft. Acceptance testing consists of a full first functional test to characterize power transfer, frequency response, linearity, phase shift, VSWR, stability, spurious emissions, group delay, and harmonic output. Next a passive (unpowered) 3-axis random vibration test is performed to levels in excess of those experienced during launch. After an abbreviated functional test verifies no change in performance resulting from vibration testing, each amplifier is subjected to a thermal vacuum environment to simulate the spacecraft's operating environment. Data are taken to verify gain stability, power output, and power consumption at all temperature plateaus. Figure 2 shows a representative set of thermal vacuum data for frequency response and gain variation with temperature. Maximum peak-to-peak gain variation across the band at 23°C is 0.25 dB with a maximum associated gain slope of 0.01 dB/MHz. Maximum peak-to-peak gain variation over temperature at any single frequency is shown to be 1.03 dB over a 23°C range. DC bias and rf drive levels are also recorded. Following successful completion of thermal vacuum testing, final functional tests identical to the first functional tests are performed.

Beyond standard acceptance testing and more extreme qualification testing, a large effort in amplifier characterization has been made.<sup>(2)</sup> Several key areas of evaluation are reported here as also reported in reference (1).

The SSPA has a greater amplitude and phase linearity than the TWTA. The amplifier is typically operated two to three dB into gain compression. A nominal associated level for the C/IM<sub>3</sub> ratio as measured by a two-tone test is -13 dBc. The power output and relative phase shift as a function of input power are shown in Figure 3. Intermodulation performance over the drive range is also shown. Noteworthy is the saturation of the intermodulation characteristic. A typical SSPA driven into hard saturation will have C/IM<sub>3</sub> performance that never exceeds a worst-case value. The derivation of the phase shift versus drive characteristic will give a static approximation to the dynamic AM-to-PM conversion performance of the SSPA. Amplitude modulation to phase modulation conversion on a single carrier and transfer between carriers are important to consider because transmission impairments such as crosstalk and increased bit error rate arise in part from these effects. A dynamic measurement of these AM-to-PM effects was made at a modulation frequency of 1 MHz. The three cases considered are depicted in Figure 4. Note the AM-to-PM conversion coefficient  $K_p$  (degrees/dB) remains below the 1°/dB level until the amplifier is completely saturated (reference Figure 3 for saturated drive level). AM-to-PM transfer ( $K_T$ ) between two equal carriers is close in magnitude to  $K_p$ . The worst-case

consideration is the transfer of modulation between two unequal carriers, which, in this case, differed by 20 dB.

The physics of a GaAs FET are such that increasing temperature results in decreasing gain and power output capability. The power distribution within the SSPA between dc input, rf output, and dissipated heat has been characterized from  $-5^{\circ}\text{C}$  to  $+55^{\circ}\text{C}$ . Results of this measurement are presented in Figure 5. It is key to note that dissipated power always decreases as the amplifier drive is increased; therefore an interesting trade-off is implied. Namely, the reliability of a GaAs FET is inversely related to channel temperature and related also, in a complex way, to voltage and current stresses incurred from increased drive.<sup>(2)</sup> A point exists at which reliability enhancement from reduced channel temperature is offset by stresses due to increased drive.

The power output and dc-to-rf efficiency are related to the high current drain bias. The results from a measurement of this relationship are given in Figure 6. Note that a 10.5-watt output is obtained for a 10V drain bias with a 2% penalty in efficiency.

The SSPA is powered by an electronic power conditioner that converts the variable spacecraft bus voltage to a regulated set of bias voltages. A pulse-width-modulator-based switching regulator of very high efficiency is employed to power the SSPA. Ripple is inherent to switching supplies, and filtering has an associated weight penalty; therefore, characterization of the SSPA ripple sensitivity is important. The relationships shown in Figure 7 express the induced sideband level around a 4-GHz carrier as a function of injected bias ripple for the three bias lines. As would be expected, the gate bias line shows greatest sensitivity. Other performance parameters have also been related to changes in bias voltage. Table 1 gives the sensitivities to bias variation of gain, power output, and relative phase for each bias line. The output power is most sensitive to fluctuations in the 8.7V line, with the  $-3.7\text{V}$  gate bias variations having greatest effect on gain and relative phase shift.

The data presented herein serve to characterize in detail the solid-state power amplifier. While the amplifier is designated an 8.5-watt unit, clearly this power output level has been selected to optimally trade off power output and linearity for increased efficiency. Specifications representing worst-case acceptable amplifier performance are tabulated along with those for a TWTA of equivalent saturated power output in Table 2. Performance advantages for the SSPA are shown in areas of linearity, phase conversion, phase shift, harmonic output, weight, and reliability. Other significant advantages of the SSPA over the TWTA include no mechanism for cathode wear-out, no outgassing or vacuum contamination leading to catastrophic failure, low voltage operation eliminating potentials for arc-over failure, and no warm-up time as required for the TWT cathode heater.

The many advantages of the SSPA have been touched upon. Further detail in this area can be found.<sup>(1)</sup> In the final analysis, improved performance and reduced distortion means the satellite that incorporates these amplifiers can handle greater traffic loading and can therefore generate greater revenue.

## **CONCLUSION**

The design and performance characteristics of the SSPA have been described. A comparison of this amplifier to a traveling-wave tube amplifier of equivalent saturated power output have shown superior performance and reliability for the SSPA. Efforts are underway to increase the margin superiority of the SSPA by improving efficiency, power output, and operational bandwidth. The next challenge is to extend the C-band SSPA technology into the 12-GHz communications band.<sup>(3)</sup>

## **REFERENCES**

- (1) Wolkstein, H. J., and LaPrade, J. N., 1982, "Solid-State Power Amplifier Replacing TWTs in C-Band Satellites," RCA Engineer, Vol. 27 No. 5, P. 7.
- (2) Dornan, B., et al., 1980, "A 4-GHz FET Power Amplifier: An Advanced Transmitter for Satellite Downlink Communications Systems," RCA Review, Vol. 41 No. 3.
- (3) Aubert, D., Dhillon, S., LaPrade, J. N., Mochalla, S., Patel, J., 1983, "Power Amplifiers Replace TWTAs in Satellite Transponders," MSN.

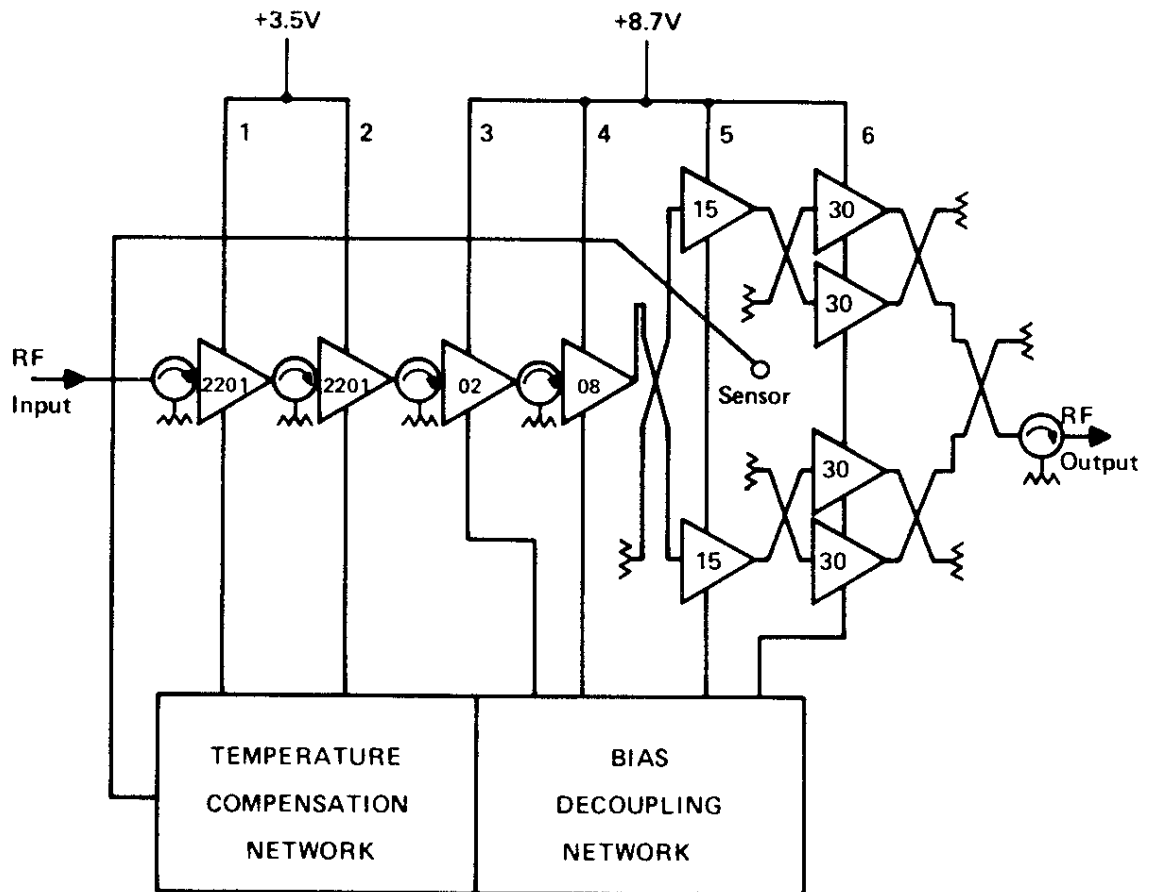
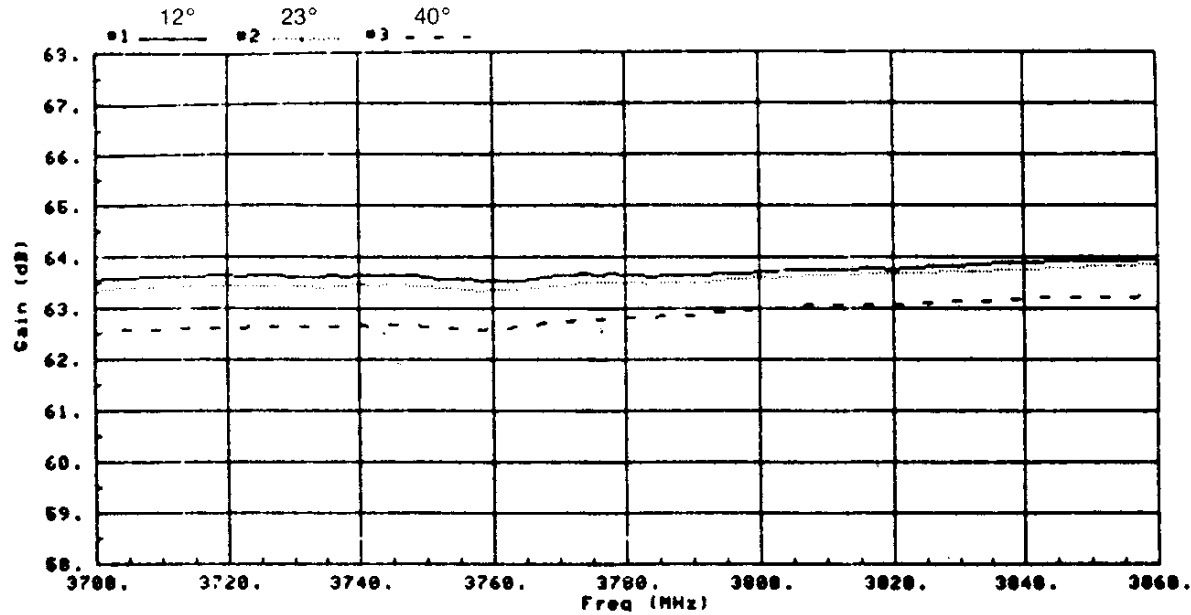


**Figure 1. SSPA Block Diagram**

SSPA-629-501-012  
 Date: 08/14 Time: 09:31:21  
 Temperature = 23 Deg C  
 Operator: D PATE

$V_d = 8.8V$   $I_d = 2906mA$   $V_g = -3.9V$   
 $I_g = -116mA$   $V_d = 3.5V$   $I_d = 23.7 mA$   
 Input power level is -36.2 dBm



Max gain variation = .250 dB  
 Max gain slope = 0.10 dB/MHz  
 Input power level is -36.2 dBm

Max gain variation = 1.03 dB

#1 \$G0124 SSPA-629-501-012 08/14 04:52:24 17 C.COLBERT  
 #2 \$G0132 SSPA-629-501-012 08/14 09:31:21 23 D PATE  
 #3 \$G0116 SSPA-629-501-012 08/13 21:57:16 40 H MOROFF

| Freq (MHz) | Gain (dB) |
|------------|-----------|
| 3700.      | 63.33     |
| 3706.      | 63.40     |
| 3712.      | 63.41     |
| 3718.      | 63.44     |
| 3724.      | 63.43     |
| 3730.      | 63.42     |
| 3736.      | 63.44     |
| 3742.      | 63.45     |
| 3748.      | 63.45     |
| 3754.      | 63.39     |
| 3760.      | 63.35     |
| 3766.      | 63.41     |
| 3772.      | 63.47     |
| 3778.      | 63.51     |
| 3780.      | 63.49     |
| 3784.      | 63.48     |
| 3790.      | 63.52     |
| 3796.      | 63.57     |
| 3802.      | 63.59     |
| 3808.      | 63.64     |
| 3814.      | 63.65     |
| 3820.      | 63.67     |
| 3826.      | 63.70     |
| 3832.      | 63.73     |
| 3838.      | 63.76     |
| 3844.      | 63.79     |
| 3850.      | 63.81     |
| 3856.      | 63.83     |

Figure 2. SSPA Frequency Response and Gain Variation with Temperature

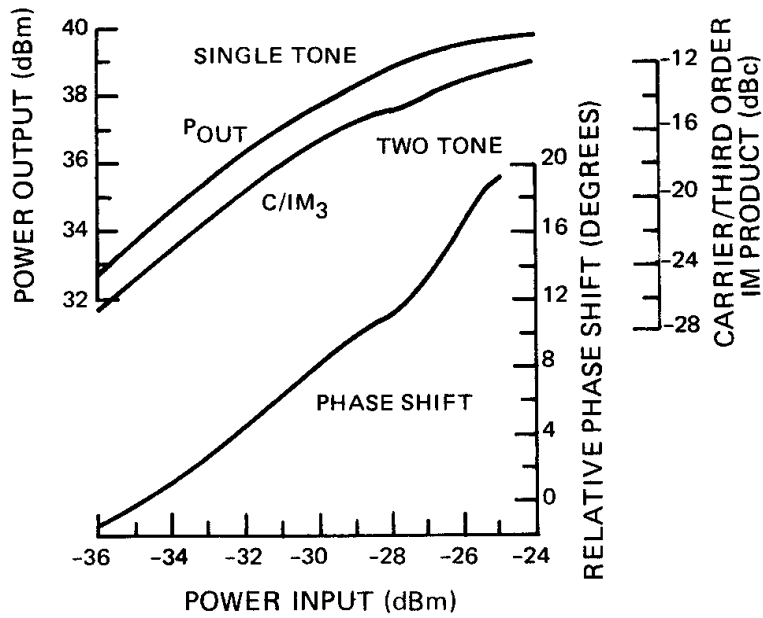


**Figure 3. SSPA Power and Phase Transfer Characteristics for a Single-Tone Input (Two-Tone C/IM<sub>3</sub> Characteristic Also Shown)**

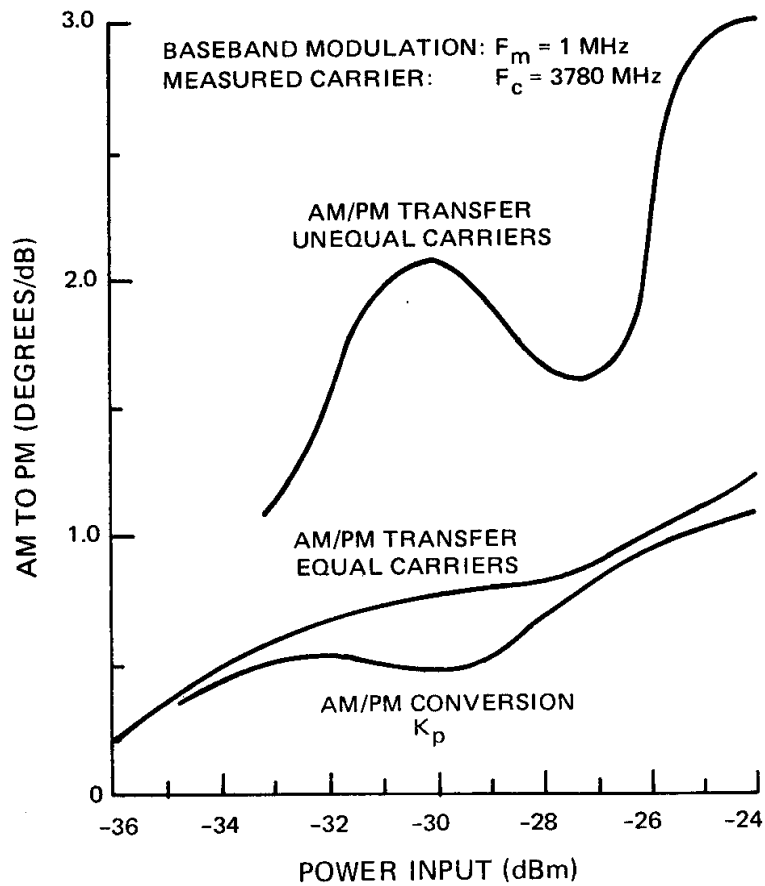


**Figure 4. AM-PM Conversion Coefficient ( $K_p$ ) and Transfer Coefficient ( $K_T$ )**

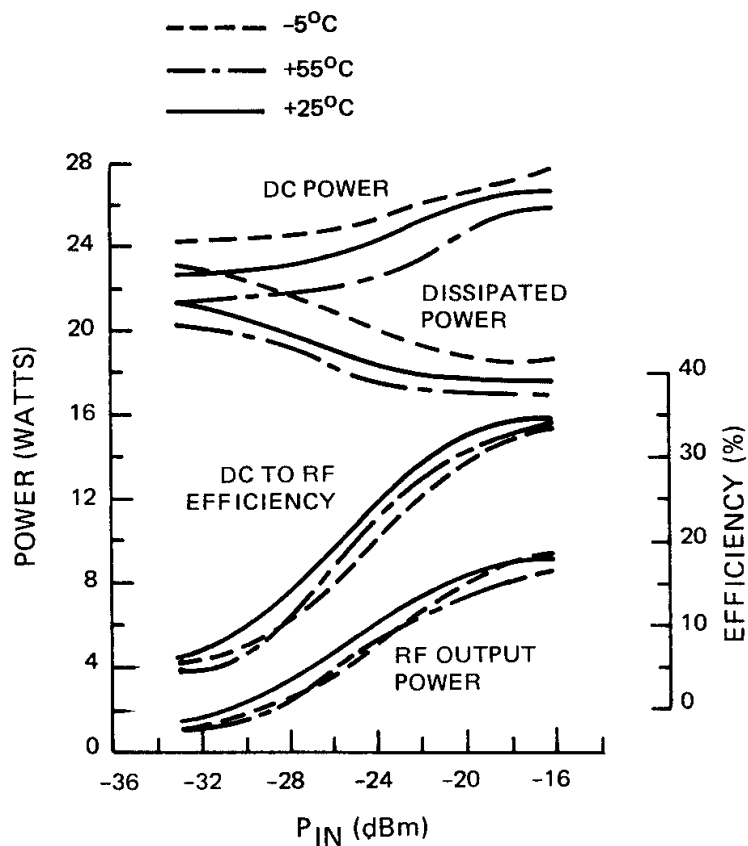


Figure 5. SSPA Power Distribution as a Function of Input Power and Temperature

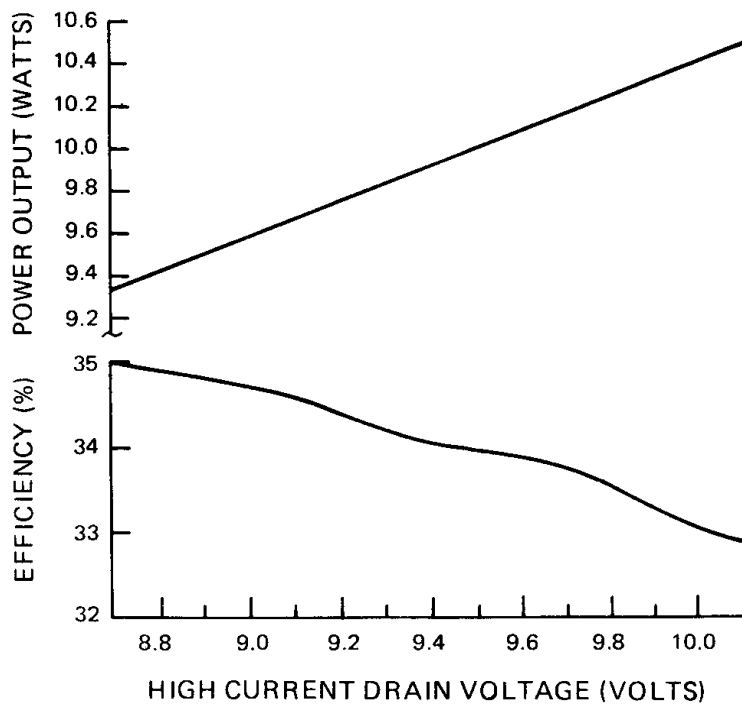


Figure 6. SSPA Power Output and Efficiency as a Function of Drain Voltage

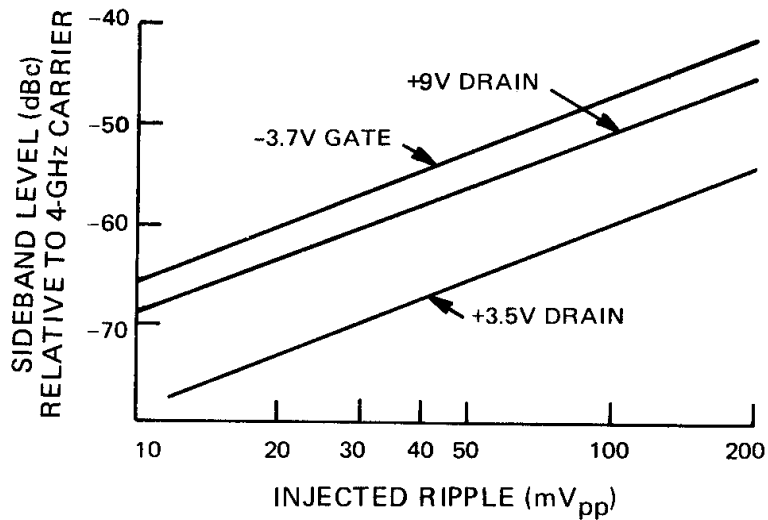


Figure 7. SSPA Ripple Sensitivity

TABLE 1. 8.5-WATT SSPA DRAIN-BIAS SENSITIVITY

|                                | <i>+8.7-V Drain</i> |             | <i>+3.5-V Drain</i>       |             |             |                           |
|--------------------------------|---------------------|-------------|---------------------------|-------------|-------------|---------------------------|
|                                | <i>10%</i>          | <i>-10%</i> | <i>Worst Case<br/>Δ Δ</i> | <i>+10%</i> | <i>-10%</i> | <i>Worst Case<br/>Δ/Δ</i> |
| <b>Small-sig-<br/>nal gain</b> | 0                   | 0.1dB       | 0.12dB                    | -0.4 dB     | +0.2 dB     | 1.15 dB/V                 |
| <b>Output<br/>power</b>        | 1.03 W              | -1.17 W     | 1.38 W/V                  | +0.03 W     | 0           | 0.086 W/V                 |
| <b>Output<br/>phase</b>        | 2.3°                | 5°          | 5.9°/V                    | 2.2°        | 1.7°        | 6.3°/V                    |
| <i>Gate-bias sensitivity.</i>  |                     |             |                           |             |             |                           |
| <i>Vg = -3.7/V</i>             |                     |             |                           |             |             |                           |
|                                |                     | <i>+10%</i> |                           | <i>10%</i>  |             | <i>Worst Case<br/>Δ Δ</i> |
| <b>Small-signal gain</b>       |                     | -0.6 dB     |                           | +0.8 dB     |             | 1.67 dB/V                 |
| <b>Output power</b>            |                     | -0.26 W     |                           | +0.1 W      |             | 0.87 W/V                  |
| <b>Output phase</b>            |                     | +4.2°       |                           | -8.2°       |             | 27.34°/V                  |

**TABLE 2. PERFORMANCE COMPARISON OF THE SSPA  
VERSUS THE TWTA**

|  | SSPA           | TWT      |
|--|----------------|----------|
| RF power   | 8.5 W          | same     |
| Frequency  | 3.7 to 4.2 GHz | same     |
| Bandwidth  | 160 MHz        | 100 MHz  |
| Power gain   | >58 dB         | same     |
| Gain compression<br>(at high-level operating<br>power) | ~2 dB          | 6dB      |
| Gain flatness  | 0.3 dB/10 MHz  | same     |
| Amplitude linearity<br>(3rd-order IMD)                 | -1 2 dBc       | -8 dBc   |
| Phase conversion (AM/PM)                               | 2°/dB          | 5°/dB    |
| Total phase shift<br>(final 10-dB drive range)         | 22°            | 45°      |
| Harmonics  | -35 dBc        | -12 dBc  |
| Efficiency   | ~33%           | 38%      |
| Maximum operating voltage                              | 10V            | 2500 V   |
| Thermal cathode-heater<br>assembly                     | none           | required |
| Weight - SSPA  | 13 oz.         | 25 oz.   |
| Weight - EPC   | 18 oz.         | 36 oz.   |
| Projected life   | 10 yrs.        | 7 yrs.   |
| Failures in 10 <sup>9</sup> hours                      | <500           | >2000    |